Journal of Computers Vol. 34 No. 5, October 2023, pp. 243-250
doi: 10.53106/199115992023103405019

Research on Zero Force Control Strategy for Flexible Joints of Industrial Robot Arms

Hong-Chao Zhou[1], Shi-Hui Dong[2], Dan-Dan Cui[2*]

[1] Tangshan Polytechnic College,
Tangshan City 063299, Hebei Province, China
Hongchao20170203@126.com

[2] School of Automation Engineering, Tangshan Polytechnic College,
Tangshan City 063299, Hebei Province, China
{shihui345432, cuidandan2018}@126.com

Received 1 August 2023; Revised 1 September 2023; Accepted 28 September 2023

Abstract. In order to achieve the control of flexible joints in industrial robotic arms, this article first establishes a zero force control mathematical model of the joint, including a simplified joint model and a joint dynamics model. Then, the fuzzy PID control algorithm is used to solve the robot mathematical model, achieving control of joint response time and speed. In order to verify the effectiveness of the joint control strategy, this article uses ABB Robot 1200 as the basic simulation model of the robot. After three-dimensional modeling of the flexible joint, it is linked to the ABB robot. Finally, the control accuracy of the control strategy is verified through a simulation environment.

Keywords: flexible joint, zero force control, PID fuzzy control

1 Introduction

Industrial robotic arms have been widely used in various industrial production processes. Due to the mature and stable technology of industrial robots, trajectory control can be achieved through programming, enabling repetitive work. In practical applications, they can replace workers to complete many tedious tasks. Human-computer interactive robots, such as surgical robots, rehabilitation robots, and collaborative robots, can move according to the guidance of external forces from natural humans, thereby completing teaching.

Zero force control of robotic arms is a functional configuration that achieves manual guidance and direct drag teaching functions, which can effectively improve the interactivity of robots as an economical and practical method. Under zero force control, natural humans only need to use small or almost zero force to drag the robot, which can make the robot adapt to external forces for movement. This is currently a research hotspot in human-machine collaborative work mode. Zero force teaching is the optimal solution for robot complex motion trajectory planning. Therefore, zero force control strategy has been widely applied in fine and personalized customization production.

Flexible robotic arms are widely studied and developed in high-precision and cutting-edge fields such as aerospace and healthcare. Although there may be uncertain disturbances during the operation of the robotic arm, such as rigid and elastic deflection during large-scale operation, and inaccurate tracking during operation, the accuracy of the robotic arm control is ensured through the combination of zero force control strategies and control methods.

The work done in this article is as follows:

1) Established a simplified model and dynamic model of the flexible joint of the robotic arm, preparing for the entry of control algorithms;

2) Completed the establishment of PID fuzzy control strategy and achieved tracking control of the speed and position of the flexible joint of the robotic arm through the strategy;

3) Realize simulation experiments of control strategies through a real 3D modeling environment.

* Corresponding Author

Chapter 2 mainly elaborates on the relevant research results, Chapter 3 is the mathematical modeling process of joints, Chapter 4 is the establishment process of control algorithms, Chapter 5 is the simulation section, and Chapter 6 is the conclusion section.

2 Related Work

Bolivar Edgar mainly studied the application of series elastic actuators to the ankle flexible joint of prostheses, and then controlled joint robustness through the coupling relationship between speed and torque. Through simulation experiments, the proposed strategy in the article can achieve the efficiency and robustness of the ankle joint [1]. Calanca Andrea mainly studied the path planning strategy of the robotic arm under zero force control when the external environment is applied to the robotic arm without affecting its accuracy. Through simulation experiments, the path planning strategy is accurate and effective [2]. Jianming Xu proposed a joint friction model of a robotic arm under sensorless conditions for robot direct teaching application scenarios, and then estimated the contact torque using the link dynamics equation to achieve zero force tracking control of the target servo motor [3]. Yan Cao proposed a sensorless robot traction teaching strategy to compensate for the irregular distribution of joint friction using the Chebyshev fitting method. The effectiveness of the algorithm was verified through experiments [4]. Fan Yang applied mixed disturbances to the external disturbance flexible joint robotic arm system and proposed an adaptive backstepping control strategy for the robotic arm flexible system. The scientific nature of the control scheme was verified through Matlab simulation analysis [5]. Ying Hong proposed a dynamic zero force control strategy for flexible joints, which combines adaptive algorithms and neural network approximators, to address the problem of parameter uncertainty and first-order unknown interference in trajectory tracking control of flexible joint robotic arms. Finally, comparative simulations were conducted in the Simulink environment to verify the superiority of the dynamic control strategy [6].

3 Dynamic Model of Flexible Joints

3.1 Establishment of Smplified Joint Model

The joint dynamics model is the foundation of zero force control for a robotic arm with flexible joints [7]. As a non rigid structure, the flexible joints are simplified and divided into two parts: the motor drive end and the load end. Establish dynamic models for each part. The dynamic model modeling of the elastic and flexible structure of a robotic arm is as follows:

$$M(\theta)\ddot{\theta}+C(\theta,\dot{\theta})+g(\theta)=T+T_w. \tag{1}$$

In the formula, θ is the torsion angle of the joint output end, $M(\theta)$ is the inertia matrix, $C(q,\dot{q})$ is the velocity term matrix related to centrifugal and Coriolis forces, $g(\theta)$ is the gravity matrix, T is the joint output end torque, and T_w is the output end torque. Dynamic modeling of the driving part of the robotic arm:

$$J\ddot{\alpha}+T_{rc}=T_m-T_f. \tag{2}$$

In the formula, J is the moment of inertia, α is the torque angle of the motor input end, T_{rc} is the flexible torque, T_m is the motor output torque, and T_f is the friction torque. The simplified joint model adopts a linear elastic mechanism, and the simplified model is:

$$T_{rc}=K(\alpha-\theta). \tag{3}$$

In the formula, K represents the flexibility of the robot joint. Considering that the load end of the joint is a nonlinear system and there are coupling characteristics between various parameters, a simple linear stiffness model is not sufficient to characterize the characteristics of joint flexibility. Therefore, it is necessary to analyze the mechanism of joint flexibility generation to achieve accurate modeling. Therefore, this article will later model and analyze the dynamics of the harmonic reducer at the load end.

3.2 Establishment of Joint Dynamics Model

The mechanical arm has reduced joint stiffness and flexibility due to the integration of harmonic reducers within its joints [8]. Therefore, considering the position, speed, and torque transmission relationships between the internal components of the harmonic reducers, a collaborative arm joint dynamics model integrating harmonic transmission is established. The joint model is shown in Fig. 1.

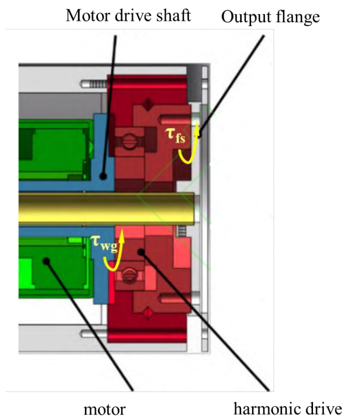

Fig. 1. Schematic diagram of joint interior

When modeling harmonic transmission, the stiffness of the wave generator and flexible wheel in harmonic transmission can be expressed by the changes in their respective angular displacement. Existing experimental results have shown that under low applied torque, the stiffness of the wave generator increases sharply with the increase of applied torque. Therefore, the stiffness model of the harmonic reducer wave generator can be expressed as:

$$\Delta\alpha_{vg} = \frac{sign(T_{vg})}{C_{vg}K_{vg}}(1-e^{-C_{vg}|T_{vg}|}). \tag{4}$$

In the formula, $\Delta\alpha_{vg}$ represents the difference in torsional angle of the robotic arm harmonic generator, T_{vg} inputs the torsional torque of the harmonic reducer, and K_{vg} and C_{vg} can be obtained through parameter identification. In the product catalog of the selected harmonic reducer, the segmented linear approximation method was used to model the flexibility of the flexible wheel. However, piecewise linear approximation has discontinuity and is imprecise due to the fact that the curve is approximated by a straight line. Therefore, a more accurate flexibility model of the flexible wheel is needed, so the stiffness of the flexible wheel is modeled as:

$$\Delta\alpha_{f} = \frac{\arctan\left(C_f T_f\right)}{C_f K_{fs}}. \tag{5}$$

In the formula, $\Delta\alpha_f$ is the difference in torsion angle of the flexible wheel, T_f is the output torque of the flexible wheel, and the constants K_{fs} and C_f depend on the properties of the harmonic reducer itself. Based on the analysis and modeling of joint harmonic transmission mentioned above, the following assumptions are made for the joint drive and transmission parts.

(1) The servo motor rotor and transmission shaft are ideal axisymmetric rigid bodies, ignoring the torsional deformation during the motor rotation process. The internal drive and transmission components of the joint en-

sure coaxiality;

(2) Servo motors are ideal power sources, ignoring motor losses;

(3) Combine the flexibility of the transmission shaft and joint output flange with the flexibility of the harmonic reducer.

Using a joint dynamics model based on the Newton Euler method, the dynamic equations for the input and output ends of the joint can be obtained as follows:

$$J_{in}\ddot{\alpha}_{in} = J_{in}\ddot{\alpha}_{vg} = T_m - T_{di} - T_{vg}$$
$$J_{out}\ddot{\alpha}_{out} = T_f - T_d - T_{load}. \tag{6}$$

In the formula, T_m represents the motor output torque, T_{di} and T_d represent the joint input and output friction torque, and T_{load} represents the complex torque.

The friction torque term only considers the viscous friction term and the simple constant Coulomb term, so the above equation can be expanded as:

$$J_{in}\ddot{\alpha}_{in} - K_m I_b = -\frac{1}{M}\left(K_{vg}\Delta\theta_{vg} + K_f\Delta\theta_f\right) - b_{in}\dot{\alpha}_{in} - f\cdot sign\dot{\alpha}_{in}$$
$$J_{out}\ddot{\alpha}_{out} - T_g = T_{out} = K_{vg}\Delta\theta_{vg} + K_f\Delta\theta_f - b_{out}\dot{\alpha}_{out} - f\cdot sign\dot{\alpha}_{out}. \tag{7}$$

Subsequently, it is necessary to identify the parameters of the joint dynamics model and convert the above equation into an identification matrix.

$$Y = \begin{bmatrix} J_{in}\ddot{\alpha}_{in} - K_m I_b \\ J_{out}\ddot{\alpha}_{out} + T_g \end{bmatrix} = \begin{bmatrix} J_{in}\ddot{\alpha}_{in} - K_m I_b \\ T_{out} \end{bmatrix}. \tag{8}$$

In the formula, J_{in} is the input rotational inertia, J_{out} is the output rotational inertia, K_m is the motor torque constant, I_b is the motor output current, T_g is the load torque, T_{out} is the joint output torque, $\Delta\alpha_{vg}$ is the harmonic generator torsion angle, and $\Delta\theta_f$ is the flexible wheel rotation angle.

4 Dynamic Model of Flexible Joints

The control system uses a PID closed-loop controller, which is a typical control method [9]. The control idea is to calculate the control quantity in the closed-loop system by proportionally amplifying, integrating, and differentiating the system error. PID controllers are widely used in industry, with stable and reliable operation and simple structure, making them one of the main control technologies in the field of industrial control. In the control schematic diagram, $r(t)$ is the expected input, $y(t)$ is the actual output of the controlled object, $e(t)$ is the error between the expected input and the actual output, and $u(t)$ is the output of the PID controller. Its value is the sum of the results of proportional, integral, and differential operations. The mathematical expression of the PID control algorithm is shown in the following equation.

$$\mathrm{u}(\mathrm{t}) = \mathrm{K}_p e(\mathrm{t}) + \mathrm{K}_\mathrm{i}\int_0^t e(t)\,dt + K_d\frac{de(t)}{dt}. \tag{9}$$

Among them, K_p, K_i, and K_d are the parameters of the proportional, integral, and differential links, respectively. Adjusting the three parameters of the *PID* control link separately will have different effects on the system parameters such as rise time, overshoot, adjustment time, and error. Build a control system control program diagram, as shown in Fig. 2.

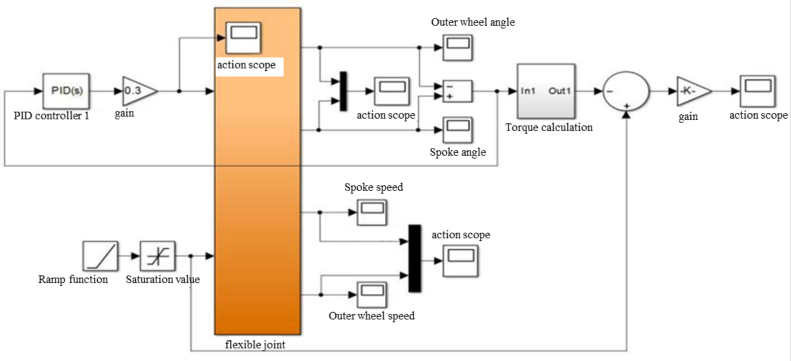

Fig. 2. System control program diagram

The PID control algorithm is applied to the flexible joint of the industrial robotic arm proposed in this article. The system design includes typical control links, which play different roles [10]. The typical control loop is the position and speed control loop. The research object of this article is the modified zero force joint of ABB industrial robot, which includes a flexible unit that mainly relies on elastic components. If only position loop control is used, when controlling the position of the robot arm, it will inevitably cause the arm joints to shake, which is the flexible unit. The system response curve without speed loop control is shown in Fig. 3.

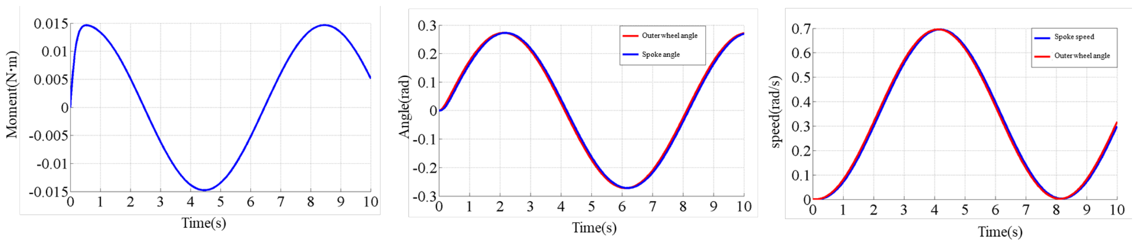

(a) Torque simulation (b) Angle simulation (c) Velocity curve

Fig. 3. Response curve

When the control loop is incomplete, the position curve of the robotic arm joint will experience shaking in the initial stage, but the curve will tend to be smooth and without shaking in the latter half. The position curve of the amplitude wheel in the joint and the position curve of the outer wheel begin to overlap, and then reach the desired position at the same speed; Due to the flexible elements at the joints, the speed of the spoke will experience significant shaking in the initial stage and gradually decay to a stable value, while the outer wheel will operate stably at a given speed, and ultimately the spoke and outer wheel will operate at the same speed.

5 Simulation Experiment Results and Analysis

The experimental phase includes force tracking experiments and zero force control experiments. The force tracking experiment mainly verifies the corresponding ability of the flexible joint to input signals after the zero force control strategy is applied to the flexible joint of the robotic arm.

5.1 Experiment on Force Tracking of Flexible Joints in Robot Arms

Build a system testing experimental platform, which mainly includes the following parts: a personal computer, equipped with NVIDIA's high-performance graphics card, with Intel's third-generation CPU, and the computer mainly running the developed data collection system; The STM32 microcontroller is a lower level controller with two main functions: on the one hand, it collects signals from the robotic arm, and on the other hand, it sends control signals from the robotic arm through the microcontroller. The flexible joint force tracking experiment is to verify the response speed and continuity of the joint. A specific force disturbance signal is input to observe the force signal fed back by the flexible joints. When the end of the flexible joints is fixed, the drag force is input to the joint in the form of a step force to obtain the force feedback at the joint, and then the force output signal of the flexible joints is collected. The experimental results are shown in Fig. 4.

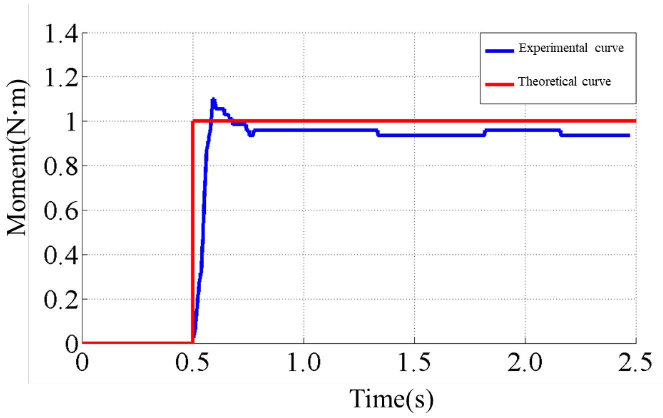

Fig. 4. Experimental diagram of flexible joint force tracking

Through the analysis of experimental results, it can be seen that the flexible joints can achieve the expected effect in following the step signal, with a fast response speed, a rise time of 0.1 s, an adjustment time of 0.25 s, an overshoot of 10%, and a steady-state error of about 5%. At the same time, it can be seen that the response curve also has certain fluctuations when stable, and the response curve is not a smooth curve, but a stepped form. The main reason for this is that the calculation of torque is indirectly obtained through the encoder.

5.2 Experiment on Zero Force Control of Robotic Arms

The zero force control experiment of the flexible joint is shown in Fig. 5. The collection system uses STM32 as the control core, mainly completing signal collection. When an external force is used as the input signal of the system, the joint provides strong feedback, and the feedback signal is collected by the collection system. Then, the corresponding algorithm is used to calculate the speed of the joint, and the torque during the joint operation is neutralized to achieve an overall torque close to 0.

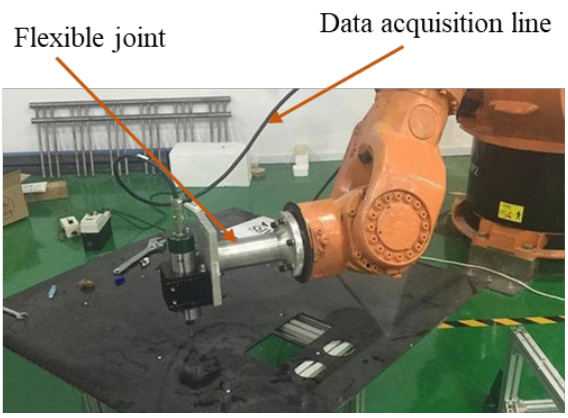

Fig. 5. Zero force experiment

Through the analysis of the experimental process, it can be seen that when the SEA joint is dragged by external force, the controller can control the motor operation through the feedback value of joint torque, and the joint speed changes with the change of torque. From the comparison in Fig. 6, it can be seen that the motor speed increases with the increase of joint torque value. When the joint torque value is zero, it can immediately stop running.

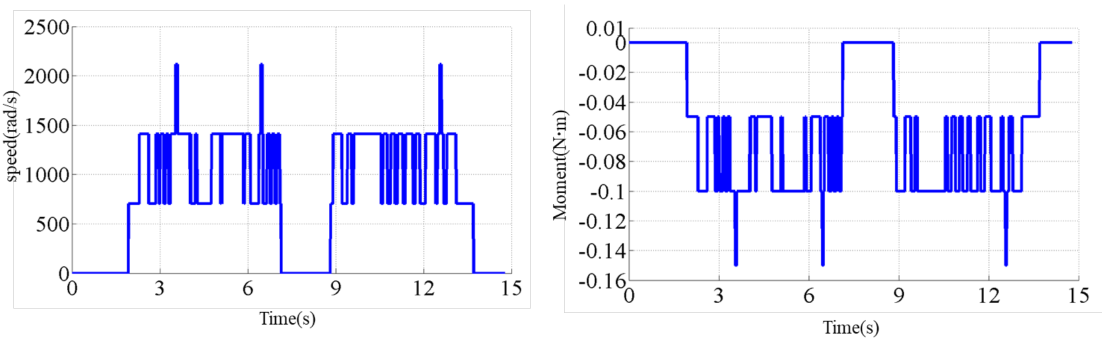

Fig. 6. Simulation run results

6 Conclusion

This article realizes the control of industrial robot joints and torque adjustment functions. The control system designed can achieve the expected design, and through experiments and data collection, it can operate under ideal data conditions. Therefore, after the analysis of this article, the following conclusion is drawn:

(1) Conclusion 1: The control system can effectively improve the teaching and control level of robots.

(2) Conclusion 2: Through SEA force tracking experiments and zero force control experiments based on SEA, the algorithm can improve the reliability and stability of control.

At the same time, this article also has shortcomings:

(1) Less than one, due to the presence of elastic components in industrial robots, slight disturbances still exist, and slight disturbances can still reduce the motion accuracy of the robot. Therefore, further research mainly aims to further eliminate disturbances.

(2) Secondly, the information collection system designed in this article has a certain delay in processing the collected signals due to insufficient programming capabilities, resulting in insufficient interpretation. Therefore, it is necessary to improve the rationality of the collection system code.

References

[1] E. Bolivar, S. Rezazadeh, T. Summers, R.-D. Gregg, Robust Optimal Design of Energy Efficient Series Elastic Actuators: Application to a Powered Prosthetic Ankle, in: Proc. International Conference on Rehabilitation Robotics, 2019.

[2] A. Calanca, P. Fiorini, Understanding Environment-Adaptive Force Control of Series Elastic Actuators, IEEE/ASME Transactions on Mechatronics 23(1)(2018) 413-423.

[3] J.-M. Xu, Z.-P. Zhao, J.-W. Dong, Free-force control of flexible robot joint system without sensors on link side, Journal of Zhejiang University (Engineering Science) 54(7)(2020) 1256-1263, 1271.

[4] Y. Cao, W.-F. Shang, X.-Y. Zhang, Research on Sensorless Force-Free Control Algorithm for Flexible Dual-Arm Medical Robot, Machinery Design & Manufacture (4)(2021) 293-295.

[5] F. Yang, L.-B. Wu, Robust adaptive tracking control of flexible joint manipulator system, Journal of Science of Teachers' College and University 43(5)(2023) 39-45.

[6] Y. Hong, H.-L. Li, J.-L. Xiao, H.-T. Liu, Simulation Study of Composite Dynamic Surface Control of Flexible-Joint Systems, Journal of Tianjin University (Science and Technology) 56(9)(2023) 973-984.

[7] H.-Z. Zhu, J.-W. Lu, X.-F. Chen, X. You, Research on minimum dynamic parameter set of multi-joint manipulator

based on random number, Journal of Hefei University of Technology (Natural Science) 44(11)(2021) 1459-1464.

[8] H. Tan, K.-L. Liu, S.-P. Kang, Research on a Inverse Dynamic Recursive Algorithm for a 6-DOF Manipulator, Machine Tool & Hydraulics 49(17)(2021) 49-53.

[9] D.-S. Luo, K.-Y. Zheng, X. Zheng, Control System of Vacuum Winding Coating Machine Based on Fuzzy Control, Techniques of Automation and Applications 40(12)(2021) 21-23.

[10] Y.-W. Wang, P.-L. Lv, S.-F. Zheng, B.-X. Zhang, S.-P. Li, X.-D. Li, Method of BP neural network PID control for flexible manipulator driven by SMA, Modern Electronics Technique 45(10)(2022) 176-181.